Influence of neutron-irradiation-induced defects on the flux pinning in $HgBa_2Ca_2Cu_3O_{8+x}$ single crystals

A. Wisniewski and R. Puzniak
Institute of Physics, Polish Academy of Sciences, aleja Lotnikow 32/46, PL-02-668 Warsaw, Poland

J. Karpinski
Laboratorium für Festkörperphysik ETH, CH-8093 Zürich, Switzerland

J. Hofer
Physik-Institut der Universität Zürich, CH-8057 Zürich, Switzerland

R. Szymczak and M. Baran
Institute of Physics, Polish Academy of Sciences, aleja Lotnikow 32/46, PL-02-668 Warsaw, Poland

F. M. Sauerzopf
Atominstitut der Österreichischen Universtitäten, A-1020 Wien, Austria

R. Molinski and E. M. Kopnin
Laboratorium für Festkörperphysik ETH, CH-8093 Zürich, Switzerland

J. R. Thompson
Department of Physics, University of Tennessee, Knoxville, Tennessee 37996-1200
and Oak Ridge National Laboratory, P.O. Box 2008, Oak Ridge, Tennessee 36831-6061
(Received 7 December 1998; revised manuscript received 10 August 1999)

The influence of fast neutron irradiation on flux pinning in $HgBa_2Ca_2Cu_3O_{8+x}$ single crystals ($T_c = 120$ K) subjected to a fluence of 5×10^{17} cm^{-2} was studied. Magnetic measurements were performed using a commercial superconducting quantum interference device magnetometer and a miniaturized torque magnetometer. In the unirradiated state, the irreversibility line (IL), plotted as $\ln(H_{irr})$ vs $\ln(1-T_{irr}/T_c)$, shows two slopes. At higher temperatures (85–100 K) the IL is described by a power-law dependence $H_{irr}(T)=H_{irr}(0)(1-T_{irr}/T_c)^{\alpha}$ with $\alpha\approx2.1$. At lower temperatures (25–60 K), a more rapid change of H_{irr} with temperature is observed, with the exponent $\alpha\approx4.8$. Irradiation shifts the IL to significantly higher magnetic fields/temperatures, where it is rather well described by a single power-law dependence with the exponent $\alpha\approx2.3$. The effective mass anisotropy $\gamma=(m_c/m_{ab})^{1/2}$, as determined from torque measurements, decreases after neutron irradiation. The shielding current density as a function of temperature up to 60 K is well approximated by the exponential dependence $j_s(T)=j_s(0)\exp(-T/T_0)$. Irradiation increases the characteristic temperature T_0 from about 5.9 K (in the as-prepared crystal) to $T_0=9.4$ K, clearly reflecting a slower decay of j_s with temperature. Neutron-generated defects significantly increase j_s and suppress the ''fishtail effect'' (an increase of j_s with magnetic field), which was present for the unirradiated crystal.

INTRODUCTION

The highest transition temperature among the high-T_c superconductors (HTSC), equal to 135 K under normal pressure, was achieved for the (optimally doped) mercury-based copper-oxide compound $HgBa_2Ca_{n-1}Cu_nO_{2n+2+x}$ with $n=3$ (Hg1223).[1] Unfortunately, the rather high value of its superconductive mass anisotropy means that the intrinsic parameters of Hg1223, which control flux pinning, are not as good as those in some other HTSC, e.g., $YBa_2Cu_3O_{7-x}$.[2–4] Nonetheless, the high T_c's of Hg-based superconductors provide a strong motivation for trying to improve the flux-pinning properties of these compounds.

To improve the performance of HTSC with the magnetic field H parallel to the c axis, which is the application limiting orientation, an important issue is strengthening the coupling between ''pancake'' vortices located in adjacent sets of CuO_2 layers (see, e.g., the recent review by Crabtree and Nelson).[5] Recently, significant improvements have been reported in the flux pinning of mercury-based ceramic samples, by partial replacement of Ba with Sr and of Hg with Re or Cr.[6–8] It was argued that at least two features of the chemically substituted compounds may enhance flux pinning: (1) the substitution of Sr for Ba significantly shortens the blocking layer by about 0.8–0.9 Å (Ref. 9) and (2) the chemical substitution at the Hg site may make the blocking layer more metallic.[10] The possibility that extended defects in a chemically substituted $HgSr_2CuO_{4+x}$ compound could act additionally as pinning centers was also explored.[11] Studies of grain-aligned $Hg_{1-x}Re_xBa_2Ca_2Cu_3O_{8+x}$ samples[12] showed

that Re substitution enhances bulk pinning at low temperatures. However, our recent studies on Re-substituted Hg1223 single crystals have shown[13] that the flux-pinning enhancements are not effective at high temperatures, where the thermal energy is large.

One can expect that strong pinning centers introduced by irradiation may be effective both at high and low temperatures and promote (re)coupling of pancake vortices. A variety of energetic particles may be used to create defects of various morphologies, including MeV protons,[14] high-energy (hundreds of MeV or more) heavy ions such as Sn, Pb, or Au,[15,16] GeV protons,[17] and neutrons.[18] Indeed, successful irradiation experiments were performed on polycrystalline $HgBa_2CaCu_2O_{6+x}$ samples using GeV protons.[19] A large upward shift of the irreversibility temperature $\Delta T_{in} \approx 25$ K was maintained in magnetic fields up to 55 kOe. Also neutron-irradiation experiments performed on $HgBa_2CuO_{4+x}$ ceramic samples were promising, indicating a possibility of large j_s enhancements and an upward shift of the IL.[20]

Irradiation with an appropriate fluence of neutrons leads to significant enhancements of the critical current density (j_c) and modifies the IL and the activation energy. At the same time it also can affect the critical temperature and basic superconducting parameters of the material. In the case of reactor neutrons, neutron energies E ranging from a few meV to several MeV are available. Many ''primary knock-on'' atoms have energies above ~10 keV (Ref. 21) that produce defect cascades. Transmission electron microscopy studies performed on $YBa_2Cu_3O_{7-x}$ (Y123) have shown that these cascades consist of highly disordered or amorphous material with thermodynamic parameters different from that of the rest of a material.[21] They have an isotropic distribution. These regions can be viewed as a type of forced phase separation generating local areas with suppressed order parameter immersed in ''good'' superconductor. In the case of Y123 superconductor, their diameter varies between 1 and 5 nm, with a mean diameter of 2.5 nm. The surrounding strain field has approximately the same size. Hence, the majority of defects extends over a spherical volume of about 5–6 nm in diameter. This size is comparable to the coherence length in the a-b plane at 77 K and it is several times larger than the distance between sets of CuO planes. These collision cascades are particularly effective pinning centers at high temperatures, where they match the diameter of the normal vortex core ($\approx 2\xi$). Lower energy recoiling atoms produce defect clusters with smaller sizes (1 nm or less). These may act as pinning centers in a way similar to that of the cascades. Recoils with the lowest energies produce Frenkel pairs, i.e., pairs of a vacancy and an interstitial atom.

In this paper we present results on the superconducting properties of single crystals of Hg1223 with augmented pinning from fast neutron irradiation. Due to the large anisotropy of this compound and all HTSC, investigations on single crystals (or aligned samples) are more conclusive than in the case of ceramic samples. Our goal was to establish to what extent large, artificial pinning centers could alter the vortex pinning properties of this compound. We have performed magnetization and torque measurements in a wide temperature-magnetic field range. In these studies we paid special attention to the position of the IL and temperature dependence of the irreversibility field. Above this line pinning vanishes due to thermally activated depinning. Hence, the position of the IL may be considered as a measure of the stability of pinning against thermal activation. We studied also the influence of neutron-generated defects on the anisotropy, the $j_s(T,H)$ dependence, and the time decay of the magnetization in the Hg1223 compound.

SINGLE CRYSTAL PREPARATION AND EXPERIMENTAL DETAILS

One of the main difficulties with the synthesis of the mercury-based compounds $Hg12(n-1)n$ is their low thermal stability. The compounds melt peritectically, but at ambient pressure they decompose before melting and the volatile components evaporate. An encapsulation of the sample with a high hydrostatic inert gas pressure was used to prevent decomposition.[22] All crystal growth experiments have been performed at Ar pressures of 10 kbar. Due to the high density of Ar gas at this pressure (>1 g/cm^3), evaporation of Hg was strongly suppressed. Single crystals were grown from a flux or from a stoichiometric melt. As a flux, $BaCuO_2$-CuO was used. The crystallization temperature was $1000 < T < 1070\,^\circ$C.

The fast neutron irradiation was performed in the central core position of the 250-kW TRIGA reactor in Vienna. The flux-density distribution is established accurately for this reactor.[23] At full reactor power, the flux density of the fast neutrons amounts to $7.6\times10^{12}\,\mathrm{cm^{-2}\,s^{-1}}$ ($E>0.1$ MeV). The sample was encapsulated in a small quartz tube, filled with helium. The temperature during irradiation was not measured, but is estimated to be below 60 °C. The crystal was subjected to a fluence of $5\times10^{17}\,\mathrm{cm^{-2}}$ ($E>0.1$ MeV).

For the magnetic measurements, two crystals of $HgBa_2Ca_2Cu_3O_{8+x}$ were selected. Each had a well-resolved transition temperature T_c of about 120 K, defined as the onset of the diamagnetic signal. The selected crystals had similar shapes approximate parallelepipeds with dimensions $0.4\times0.4\,\mathrm{mm^2}$ in the a-b plane and a thickness of about 20 μm along the c axis. Magnetization measurements of the $M(H)$ dependence were conducted over a wide temperature range using a commercial Quantum Design MPMS 5 magnetometer. All measurements were performed in the magnetic field geometry $H \| c$ using the magnetometer's reciprocating sample oscillation mode at 1 Hz frequency with a scan length of 2 cm. The accuracy of the magnetic moment determination was about 5×10^{-7} emu. Measurements of the irreversible magnetization generally probe the conduction of current at very low electric field levels, i.e., with very low dissipation. Unfortunately, due to the small sizes of the crystals we were not able to perform transport measurements, which normally probe current conduction at considerably higher power dissipation.

The irreversibility field H_{irr} was determined as the field of the first resolved difference between lower and upper branches of the hysteresis loop with a criterion of 10^{-6} emu. For our samples, this corresponds to a magnetization difference of 0.3 G and to a current density criterion of 200 A/cm^2, with the magnetic field applied along the c axis. In all magnetization relaxation measurements, the following procedure was applied. In order to measure relaxation on the increasing branch of the hysteresis loop, the sample was cooled in zero

field to a given temperature, then the field was increased to the required value and the decay of magnetic moment was measured for 2.5 h. In order to perform measurements on the decreasing branch, the sample was cooled to the given temperature in the maximum available field of 55 kOe, then the field was decreased to the required value and the relaxation was measured.

Torque magnetization measurements have been performed using a miniaturized torque sensor.[24,25] The magnetic torque τ acting on a sample with *anisotropic* magnetic moment **m** in an applied homogeneous field **H** is given by $\tau = \mathbf{m} \times \mathbf{H}$. In an angular dependent measurement, τ is recorded as a function of the angle θ between **H** and the sample's a-b plane. From the signals recorded in clockwise $[\tau_+(\theta)]$ and counterclockwise $[\tau_-(\theta)]$ direction of a rotation, one can obtain the reversible torque $\tau_{\mathrm{rev}}(\theta) = 1/2[\tau_+(\theta) + \tau_-(\theta)]$ and the irreversible torque $\tau_{\mathrm{irrev}}(\theta) = 1/2[\tau_+(\theta) - \tau_-(\theta)]$. The reversible torque is a measure of the equilibrium intrinsic properties of the sample, whereas the irreversible torque is due to the pinning of vortices and thus is related to the sample microstructure. For HTSC demagnetization effects due to the reversible moment can be neglected in fields much larger than the lower critical field; then the only physical quantity responsible for the angular dependence of the reversible torque is the intrinsic anisotropy $\gamma = (m_c/m_{\mathrm{ab}})^{1/2}$. Therefore, magnetic torque measurements are a particular convenient way to determine γ. Due to the large anisotropy, the screening currents flow mainly in the a-b plane and **m** is directed along the c axis for almost all field orientations θ. Therefore, the magnetic torque continuously increases when the field is rotated away from the c axis. Only when **H** gets very close to the a-b plane **m** starts to flip and the torque decreases. The angle θ_m where the torque reaches its maximum is a measure of the anisotropy γ. If one is not too close to T_c, the angular-dependent torque is well described by a three-dimensional (3D) anisotropic London model.[26] A fit to the angular-dependent reversible data using this model directly yields the effective mass anisotropy γ.

RESULTS AND DISCUSSION

We focus on the impact of neutron-generated microstructures on superconducting properties of Hg1223 single crystals. Thus we compare and contrast their vortex state features, both irreversible and irreversible. We consider first the material at lower temperatures and magnetic fields, where macroscopic circulating currents cause the magnetic response to be irreversible. For both as-prepared crystals, the hysteresis loops $M(H)$ are symmetric with respect to the reversible magnetization at all investigated temperatures. As is evident in Fig. 1, the lower and upper branches of the loop are strongly field dependent over the entire temperature range. In particular, there is no flat part in the M_{irr}-H dependence (specifically with $M_{\mathrm{irr}} \approx 0$ for the decreasing field branch); this means that surface barrier effects are not important here. The circulating currents are distributed throughout the volume of the sample, rather than just on its surface. Hence, the width of the hysteresis loop is determined by bulk pinning. We mention this, since in the case of magnetically aligned Hg1223 materials, a strong influence of surface barrier effects on flux pinning was observed.[12,27]

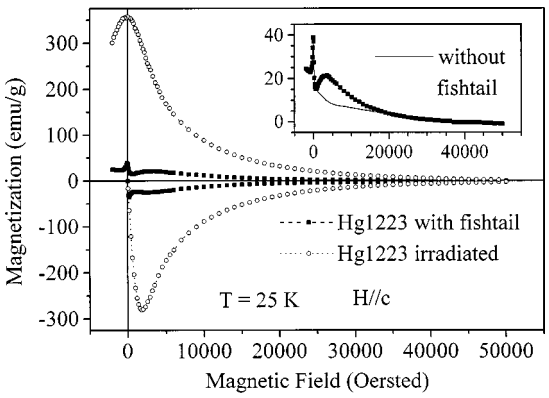

FIG. 1. Comparison of the $M(H)$ loops at 25 K for $HgBa_2Ca_2Cu_3O_{8+x}$ single crystals before and after fast neutron irradiation. Inset: the difference between the decreasing branches of the hysteresis loop for unirradiated single crystals, with and without a fishtail.

One of the as-grown crystals studied here exhibits a fishtail effect, a second maximum in the width of hysteresis loop. This feature is clearly visible in the temperature range 25–50 K, see Fig. 1. It is much less pronounced in the higher temperature range 50–80 K, and not observed above 80 K. The second peak begins to develop in relatively low fields of about 2 kOe and its position is rather temperature independent. The second crystal has no fishtail, so the $M(H)$ curves clearly differ in low magnetic fields. However, in higher fields close to the irreversibility field the magnetic responses for the two crystals are quite similar, as seen in the inset in Fig. 1. After precharacterization, the first crystal (with a fishtail) was neutron irradiated. Its critical temperature and the width of the superconducting transition were changed insignificantly by the irradiation, less then 0.5 K.

Irradiation-induced defects strongly impacted on the flux pinning. For the applied fluence, the density of cascades is of the order of $10^{22}\,\mathrm{m}^{-3}$,[21] hence, the mean separation of the cascades is about 50 nm. Due to their relatively high density and ''suitable'' sizes they are mainly responsible for observed changes in flux-pinning properties. At all temperatures, the width of the hysteresis loops increased significantly. A comparison of the $M(H)$ loops at $T = 25\,\mathrm{K}$ before and after the irradiation is shown in Fig. 1. Note, too, that the fishtail disappeared. The pinning mechanism responsible for this effect is suppressed or masked by the strong pinning of the irradiation-induced defects. The addition of strong vortex-pinning sites is particularly notable at intermediate and high temperatures. Figure 2 shows that the relative width of the hysteresis loops, i.e., the increase of the shielding current density, is more pronounced at higher temperatures. For example, at 40 K in a field of 10 kOe, the enhancement factor $\Delta M_{\mathrm{irrad}}/\Delta M_{\mathrm{unirrad}}$ is about 20. At higher temperatures, e.g., $T = 60\,\mathrm{K}$, the falloff of the current density with increasing magnetic field is significantly slower after neutron irradiation (see the inset in Fig. 2). Hence, the neutron-induced defects, due to their relatively large sizes, are quite effective pinning centers at temperatures close to 77 K.

Figure 3 presents the shielding current density j_s determined from the width ΔM of the hysteresis loops in a magnetic field of 6 kOe. For this, the critical state model was

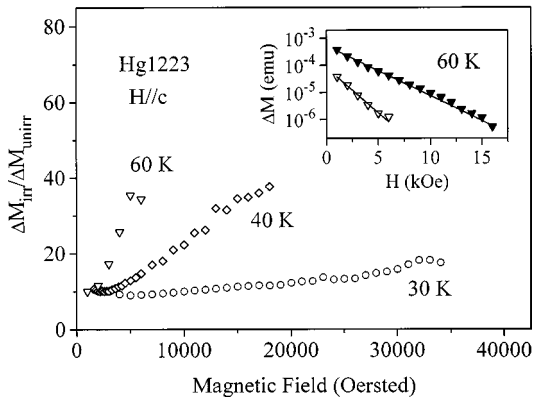

FIG. 2. The increase of the width of the hysteresis loops, i.e., the increase of the shielding current density, as a result of neutron irradiation $\Delta M_{\mathrm{irrad}}/\Delta M_{\mathrm{unirrad}}$ at temperature of 30, 40, and 60 K for a $HgBa_2Ca_2Cu_3O_{8+x}$ single crystal. In the inset field dependence of the width of $M(H)$ loop at temperature of 60 K, for unirradiated (open triangles) and for irradiated (closed triangles) is shown.

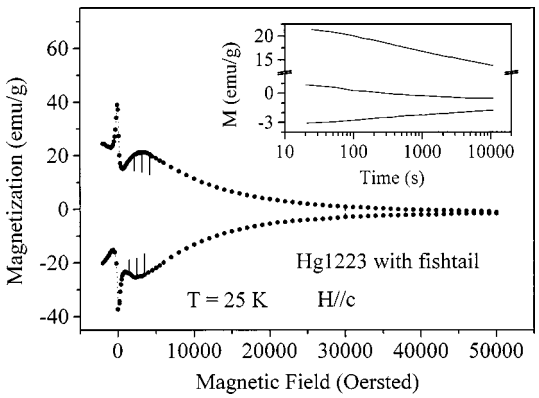

FIG. 4. The $M(H)$ loop at 25 K for a $HgBa_2Ca_2Cu_3O_{8+x}$ single crystal. The relaxation of the magnetization during the time interval of 10^4 s is indicated. In the inset the relaxation as a function of $\ln t$ is shown in the field of 3.2 kOe for the decreasing field branch and in the field of 30 kOe for both increasing and decreasing field branches of the hysteresis loop.

used, which provides that $j_s = 15\Delta M/r$, where $2r$ is the edge length of the square crystal. This relation assumes that magnetic flux penetrates to the center of the crystal, which is the clearly the case for the data presented. For both materials, j_s falls off quasiexponentially with temperature over the range 5–60 K, as is evident in the figure. The approximate temperature dependence arises from thermally activated depinning of vortices[28] that reduces the gradient of the flux density. The parameter T_0 which characterizes the decrease of j_s with temperature, increases from about 5.9 K before irradiation to about 9.4 K after irradiation. This demonstrates that neutron-generated defects significantly improve the current-carrying properties of Hg1223.

To gain insight into the pinning and dynamics of vortices in the Hg1223, we have studied the relaxation of magnetization at temperature of 25 K. As shown in Fig. 4, the unirradiated crystal has a clearly visible fishtail at this temperature. We speculate that this feature arises from a softening of the vortex system, when pancake vortices in adjacent layers start to lose their correlation. This occurs in fields larger than the crossover field H_{cr} which is particularly evident in the IL, as

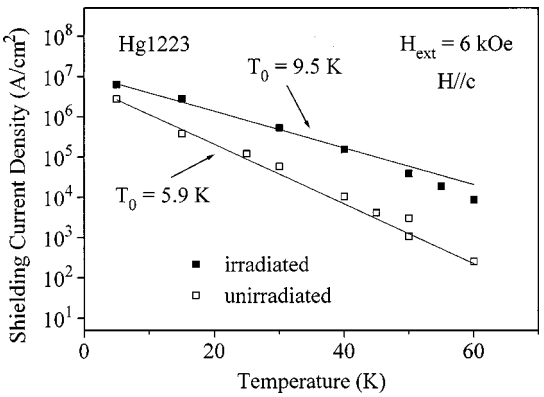

FIG. 3. The shielding current density for a $HgBa_2Ca_2Cu_3O_{8+x}$ single crystal before and after neutron irradiation determined in a magnetic field of 6 kOe. The temperature dependence of j_s is well described by the equation: $j_s(T) = j_s(0)\exp(-T/T_0)$, for the crystals before and after neutron irradiation.

discussed latter. The softer vortex system is pinned with a higher efficiency, which leads to an increase of the irreversible signal. This picture is supported by the fact that the second peak begins to develop in fields of the order of H_{cr} and its position is rather temperature independent. Neutron irradiation-induced defects prevent the loss of correlation hence, no fishtail is observed after irradiation. In order to establish the influence of the relaxation on the anomalous shape of the $M(H)$ loop, we performed measurements in magnetic fields slightly below, at, and slightly above the second maximum. For the lower branch, the values of these fields are 1.5, 2.5, and 3.5 kOe, respectively. Measurements in a field of 30 kOe were also performed. The relaxation of the magnetization is quite pronounced. After 10^4 s, the magnetization decreased by about 21%, 27%, 32%, and 42% in field of 1.5, 2.5, 3.5, and 30 kOe, respectively. For the upper branch we obtained very similar decreases. Hence, relaxation increases systematically with increasing magnetic field. The same tendency is observed for the normalized creep rate defined as $R = d(\ln j_s)/d(\ln t)$, where j_s denotes the shielding current density. The corresponding R values are 0.022, 0.025, 0.028, and 0.056, respectively. As seen in Fig. 4, the fishtail effect is smeared out with time; after an interval of 10^4 s the second peak vanishes or is shifted to considerably lower fields. This change of behavior is associated with lower levels of current densities, which reduces the Lorentz force on the vortex system. As one can see in the inset of Fig. 4, the decay of the magnetization is well described by a logarithmic time dependence.

Following the irradiation, the relaxation of the magnetization, which is still logarithmic in time (see Fig. 5), is even more pronounced. After 10^4 s the magnetization in field of 2.5, 3.5, and 30 kOe decreased by about 31%, 34%, and 53%, respectively, corresponding to logarithmic rates $R = 0.028$, 0.030, and 0.049. Hence, we can conclude that neutron-induced defects that increase the current density j_s (and significantly elevate the position of the IL, see below) do not significantly reduce the fractional flux creep rate at low temperatures. However, one must bear in mind that the absolute level of current densities is far higher in the presence of the artificially created pinning centers. At the same

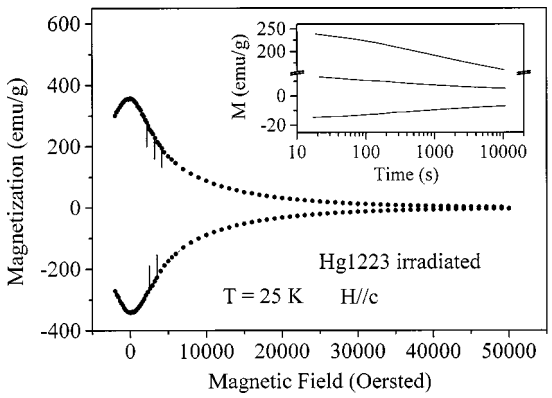

FIG. 5. The $M(H)$ loop at 25 K for a $HgBa_2Ca_2Cu_3O_{8+x}$ single crystal after irradiation. The relaxation of the magnetization during the time interval of 10^4 s is indicated. In the inset the relaxation as a function of $\ln t$ is shown in the field of 3.2 kOe for the decreasing field branch and in the field of 30 kOe for both increasing and decreasing field branches of the hysteresis loop.

current densities as those realized in the unirradiated crystal, the decay rate would be vanishingly small.[29]

With increasing temperature and magnetic field, the ability of superconductor to conduct macroscopic current deteriorates and becomes immeasurably small at the irreversibility line. Figure 6(a) shows the temperature dependence of the irreversibility field for Hg1223 with the magnetic field applied along the c axis. Included are results for both of the unirradiated crystals (with and without the fishtail effect) and for the irradiated crystal. As one can see, the presence or absence of the fishtail effect has practically no influence on the position of the irreversibility line. In this standard plot of $\ln(H_{\rm irr})$ vs $\ln(1-T_{\rm irr}/T_c)$, the data for the unirradiated crystals form two linear segments with different slopes. At higher temperatures (85–100 K) and in *lower* magnetic fields, the IL shows a power-law dependence $H_{\rm irr}(T) = H_{\rm irr}(0)(1-T/T_c)^{\alpha}$ with an exponent $\alpha \approx 2.1$. This is very close to the value $\alpha = 2$ predicted for the conventional melting of the three-dimensional vortex lattice. At lower temperatures (25–60 K) and in *higher* fields, a more rapid change of $H_{\rm irr}$ with temperature is observed. The IL can again be approximated by a power-law dependence, but with a much larger exponent $\alpha \approx 4.8$. This increase of the exponent α for higher fields may be interpreted as an indication of increasing two-dimensionality of the system at lower temperatures. The crossover in the slopes takes place at a field of $H_{\rm cr} \approx 3$ kOe, at $T_{\rm cr} \approx 66$ K. In the fields lower than $H_{\rm cr}$, pancakes couple into vortices and form a three-dimensional system. According to Blatter *et al.*,[28] a vortex system with weak pinning crosses over from 2D to 3D behavior at a field $\mu H_{\rm cr} \approx \Phi_0/(s^2\gamma^2)$, where Φ_0 is the flux quantum and s is the spacing between the sets of CuO sheets. This expression with $H_{\rm cr} = 3$ kOe provides the preliminary estimate that $\gamma \approx 50$ for the underdoped Hg1223 crystal studied here. As discussed below, refined determinations of γ have been obtained from torque magnetometry studies.

The addition of neutron-generated defects changes the character of the IL. The IL not only shifts to higher values, but the two-segment boundary, with exponents $\alpha = 4.8$ below $T_{\rm cr}$, and $\alpha = 2.1$ above $T_{\rm cr}$ are replaced by a single boundary with slope $\alpha \approx 2.3$. This exponent is nearly the same as that

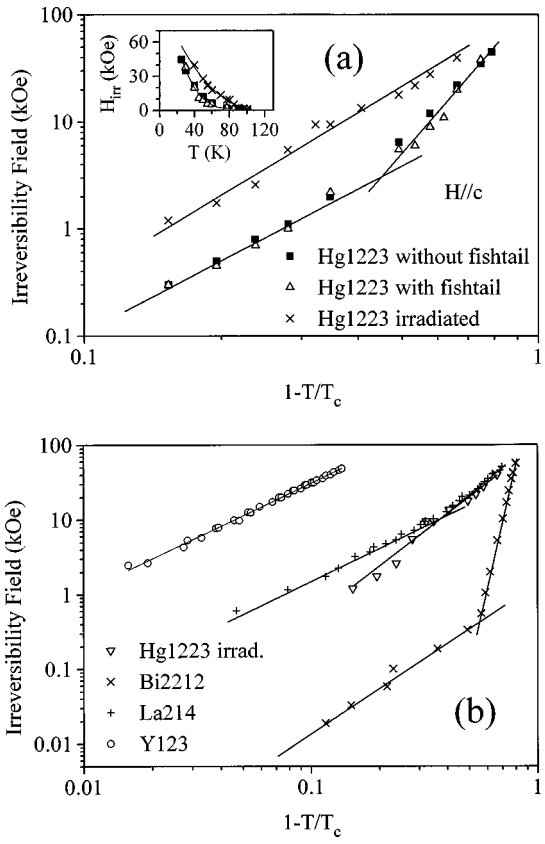

FIG. 6. (a) Comparison of the irreversibility line for a $HgBa_2Ca_2Cu_3O_{8+x}$ single crystal before and after neutron irradiation presented on a logarithmic scale of $(1-T/T_c)$. In the inset the IL's are presented for the real temperature scale. (b) Comparison of the irreversibility line for $YBa_2Cu_3O_{7-x}$, $La_{1.86}Sr_{0.14}CuO_4$, $Bi_2Sr_2CaCu_2O_{8+x}$ single crystals and for a neutron-irradiated $HgBa_2Ca_2Cu_3O_{8+x}$ single crystal.

observed at higher temperatures before irradiation. Following the interpretation of the crossover given above, this would imply a more three-dimensional character of the flux line lattice (FLL) in the whole observed temperature range. This may arise from a forced alignment of the pancakes due to the large pinning centers. As the defect cascades extend over three or four sets of CuO_2 layers, the pancakes in their vicinity are aligned over that distance, which will cause an extended alignment by the stronger in-plane interaction of the pancakes. If the density of large defects is large enough, quasi three-dimensional behavior of the FLL can be enforced for basically two-dimensional superconductivity.

Figure 6(b) presents a comparison of the irreversibility lines for $YBa_2Cu_2O_{7-x}$,[30] $La_{1.86}Sr_{0.14}CuO_4$ (La214),[31] $Bi_2Sr_2CaCu_2O_{8+x}$ (Ref. 32) single crystals and for the irradiated $HgBa_2Ca_2Cu_3O_{8+x}$ single crystal. The IL of the irradiated Hg1223 crystal is located at significantly higher magnetic fields and at higher temperatures than that of $Br_2Sr_2CaCu_2O_{8+x}$—a compound with much higher anisotropy. Comparing the IL's for irradiated Hg1223 crystal and La214 crystal (anisotropy $\gamma \approx 20$) shows that their positions are very similar for $T/T_c < 0.7$. On the other hand, the IL of Y123 ($\gamma \approx 6$) is clearly the highest of these materials; at 77 K, the irreversibility field for irradiated Hg1223 is $H_{\rm irr} \approx 10$ kOe ($H_{\rm irr} \approx 2$ kOe before irradiation), whereas Y123 has $H_{\rm irr} \approx 50$ kOe.

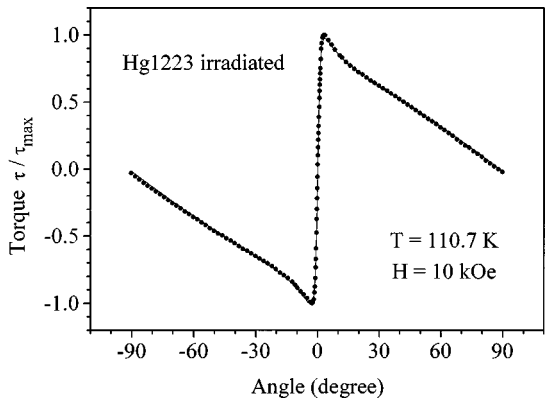

FIG. 7. Reversible angular-dependent torque signal for a fast neutron-irradiated $HgBa_2Ca_2Cu_3O_{8+x}$ single crystal at a temperature of 110.7 K determined in a magnetic field of 10 kOe. The angle of 0° corresponds to the in-plane magnetic field, while the angle of 90° corresponds to the magnetic field applied along the *c* axis of the crystal. The data (full circles) are described well within a three-dimensional anisotropic London model. A least-square fit (continuous line) yields an effective mass anisotropy $\gamma = 41 \pm 1$. For clarity not all measured data points are shown.

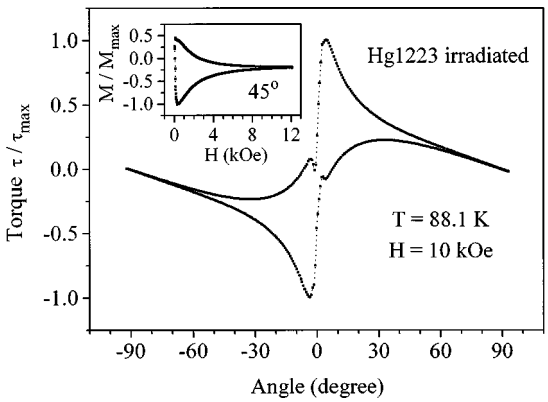

FIG. 8. The irreversible torque signal for fast neutron-irradiated $HgBa_2Ca_2Cu_3O_{8+x}$ at a temperature of 88.1 K measured in a magnetic field of 10 kOe. A pronounced irreversibility is observed for fields applied almost parallel to the *a*-*b* plane. The inset shows the field dependence of the magnetization at the same temperature. The magnetization is determined from a field-dependent torque measurements at a fixed angle of 45° out of the *a*-*b* plane.

With these changes in the irreversible properties of the material, it is clearly important to establish what changes, if any, occur in its equilibrium properties. One of the most important controlling parameters is the mass anisotropy γ, which was measured by torque magnetometry. For this, two small pieces ($0.15 \times 0.15\,mm^2$ in the *a*-*b* plane), one taken from the irradiated crystal and one from the unirradiated crystal without fishtail, were studied using a miniaturized piezoresistive torque sensor.[24] For the unirradiated crystal, we found $\gamma \approx 60$. There were no torque measurements performed on the crystal with a fishtail before the neutron irradiation. However, prior to irradiation the sample with a fishtail (1) had the same T_c and exhibited the same reversible behavior as the sample without a fishtail and (2) it had a very similar IL, including similar slopes α and the same crossover field H_{cr} [cf Fig. 6(a)]. This allows the conclusion that the sample with fishtail also had an anisotropy $\gamma \approx 60$ before the irradiation. If one takes into account that the studied crystals are underdoped, this value is ''reasonable'' when compared with the anisotropy value $\gamma \approx 44$ that was determined[22] for an optimally doped Hg1223 crystal.

Figure 7 shows the angular dependence of the torque for the irradiated crystal in an applied field $H = 10\,kOe$ at $T = 110.7\,K$. From the measurements, the anisotropy is found to be $\gamma = 41(1)$. This value is clearly smaller than the anisotropy $\gamma \approx 60$ deduced from torque measurements on the unirradiated sample (without fishtail). Hence, we can conclude the neutron irradiation causes a remarkable decrease in the anisotropy. This is consistent with the observed more 3D character of the IL. The anisotropy of the underdoped crystal ($T_c = 120\,K$) after irradiation is even slightly smaller then the anisotropy of an optimally doped Hg1223 crystal. Qualitatively, the observed reduction in the anisotropy should increase the 2D-3D crossover field H_{cr} and elevate the IL. For the irradiated crystal with lower γ, the expression $\mu H_{cr} \approx \Phi_0/(s^2\gamma^2)$ predicts that $H_{cr} \approx 7$ kOe; examination of the IL data in Fig. 6(a) implies, however, that the crossover (if it exists) must lie at much higher fields. This apparent discrepancy can be understood by recalling that the theoretical expression deals with weak pinning, whereas the irradiated crystal contains large defects. It appears that these defects help to maintain a more 3D-like vortex structure, a phenomenon somewhat similar to the observed effects of columnar defects in $Bi_2Si_2CaCu_2O_{8+x}$ single crystals.[33] The Josephson plasma resonance study showed that the apparent interlayer coupling was increased and both trapped and untrapped vortices were aligned by the columns via vortex-vortex interactions. The authors of Ref. 33 concluded that even a small number of columnar defects plays an important role in the controlling the properties of the vortex system. One can speculate from the present work that neutron-generated extended defects significantly affect the nature of the vortex system in this Hg-cuprate superconductor.

A reduced anisotropy in irreversible properties has been observed in neutron-irradiated $YBa_2Cu_3O_{7-x}$ single crystals.[34,35] In these papers, changes in the shielding currents and in the position of the IL after sequential irradiation were studied, for both the $H \| c$ and $H \| ab$ orientations. A qualitative model based on the layered structure of the system and the nature of the defects introduced by neutron irradiation was developed.[35] It was pointed out that at low densities of large defects (cascades), the reversible properties of the superconductor are determined by the density of small defects, which influence the properties of the material by isotropic scattering of the electrons. This leads to a smearing of the layered structure of the superconducting properties and hence to reduction of the anisotropy. At higher fluences (comparable with the fluence used in this experiment) bulk disorder increases, thereby reducing the anisotropy of the crystal properties.

Figure 8 shows the torque vs angle for the irradiated crystal at $T = 88.1\,K$, in an applied field $H = 10\,kOe$. A pronounced irreversibility is found for angles close to $\theta = 0°$ (field orientation near the *a*-*b* plane). The appearance of the irreversibility in the angular dependence of the torque is related to the appearance of the irreversibility in the field dependence of magnetization. Upon turning the applied field towards the *a*-*b* plane of the sample, the *c* component of the

field, $H\|c$, is reduced. Since the value of the irreversible signal in highly anisotropic cuprates is mainly determined by this component, turning the field towards the a-b plane in a torque measurement has the same effect as a lowering the applied field in a measurement with $H\|c$, leading to an increase of the irreversible signal.[36] The observed behavior is expected for isotropic pinning. For anisotropic pinning, as in the presence of columnar defects, the irreversibility should be especially evident for the field orientations where the pinning is most effective, e.g., parallel to the columns.[37] The inset in Fig. 8 shows the magnetization as a function of the field, derived from a field-dependent torque measurement at a fixed angle of 45° from the a-b plane. Since the time constant in torque measurements is much shorter than the time scale of superconducting quantum interference device (SQUID) magnetization measurements, the irreversibility is more pronounced than that in the quasi-static SQUID measurements, where the system has more time to relax. The small bump observed at $\theta \approx -2°$ in the $\tau_+(\theta)$ branch and at $\theta \approx +2°$ in the $\tau_-(\theta)$ branch, respectively, arises most probably from the lock-in effect. The lock-in effect reduces pinning effects when the field is rotated towards the a-b plane of the sample, whereas it enhances pinning effects, when the field is turned out of the a-b plane.

CONCLUSIONS

Our studies show that neutron-irradiation-induced defect structures significant influence the properties of $HgBa_2Ca_2Cu_3O_{8+x}$ single crystals. The irradiation not only enhances the flux pinning, as expected, but it also significant decreases the effective mass anisotropy γ. Torque measurements, which provide an unambiguous and direct way to measure the anisotropy, show that γ decreased from ≈ 60 prior to irradiation, to $\gamma \approx 41$ after irradiation. This value is smaller than that of optimally doped Hg1223. Neutron-generated defects increased the shielding current density and reduced its falloff with temperature. The fishtail feature disappeared with irradiation, as did the crossover in the irreversibility line, with its two linear segments. This indicates that defect cascades are able to correlate several pancake vortices and ''force'' them to behave rather in a 3D than in a 2D way. Furthermore, the IL of the irradiated crystal has an exponent α near 2, which is indicative of linelike vortices. The influence of neutron irradiation-induced defects is particularly pronounced at elevated temperatures near 77 K, which is important from the viewpoint of applications.

ACKNOWLEDGMENTS

This work was partially supported by the Polish Government Agency KBN under contract No. 722P039509 and by Swiss National Science Foundation. The Oak Ridge National Laboratory is managed by Lockheed Martin Energy Research Corp. for the US Department of Energy under Contract No. DE-AC05-96OR22464. Two of us (A.W. and J.R.T.) acknowledge support by NATO Cooperative Research Grant HTECH CRG 974620.

[1] A. Schilling, M. Cantoni, J. D. Guo, and H. R. Ott, Nature (London) **363**, 56 (1993).
[2] U. Welp, G. W. Crabtree, J. L. Wagner, D. G. Hinks, P. G. Radaelli, J. D. Jorgensen, J. F. Mitchell, and B. Dabrowski, Appl. Phys. Lett. **63**, 693 (1993).
[3] A. Umezawa, W. Zhang, A. Gurevich, Y. Feng, E. E. Hellstrom, and D. C. Larbalestier, Nature (London) **364**, 129 (1993).
[4] P. Estrela, C. Abilio, M. Godinho, J. L. Tholence, and J. J. Capponi, Physica C **235-240**, 2731 (1994).
[5] G. W. Crabtree and D. R. Nelson, Phys. Today **50** (4), 38 (1997).
[6] J. Shimoyama, S. Hahakura, R. Kobayashi, K. Kitazawa, and K. Kishio, Physica C **235-240**, 2795 (1994).
[7] J. Shimoyama, K. Kishio, S. Hahakura, K. Kitazawa, K. Yamaura, Z. Hiroi, and M. Takano, in *Advances in Superconductivity VII*, edited by K. Yamafuji and T. Morishita (Springer-Verlag, Tokyo, 1995) p. 287.
[8] J. Shimoyama, S. Hahakura, K. Kitazawa, K. Yamafuji, and K. Kishio, Physica C **224**, 1 (1994).
[9] O. Chmaissem, J. D. Jorgensen, K. Yamaura, Z. Hiroi, M. Takano, J. Shimoyama, and K. Kishio, Phys. Rev. B **53**, 14 647 (1996).
[10] K. Yamaura, J. Shimoyama, S. Hahakura, Z. Hiroi, M. Takano, and K. Kishio, Physica C **246**, 351 (1995).
[11] O. Chmaissem, D. N. Argyriou, D. G. Hinks, J. D. Jorgensen, B. G. Storey, H. Zhang, L. D. Marks, Y. Y. Wang, V. P. Dravid, and B. Dabrowski, Phys. Rev. B **52**, 15 636 (1995).
[12] L. Fabrega, B. Martinez, J. Fontcuberta, A. Sin, S. Pinol, and X. Obrados, Physica C **296**, 29 (1998).
[13] R. Puzniak, J. Karpinski, A. Wisniewski, R. Szymczak, M. Angst, H. Schwer, R. Molinski, and E. M. Kopnin, Physica C **309**, 161 (1998).
[14] E. Mezzetti, S. Colombo, R. Gerbaldo, G. Ghigo, L. Gozzelino, B. Minetti, R. Cherubini, and A. Wisniewski, in *Fourth Euro Ceramics*, edited by A. Barone, D. Fiorani, and A. Tampieri (Gruppo Editoriale Faenza Editrice, Faenza, 1996), Vol. 7, p. 349.
[15] L. Civale, A. D. Marwick, T. K. Worthington, M. A. Kirk, J. R. Thompson, L. Krusin-Elbaum, Y. Sun, J. R. Clem, and F. Holtzberg, Phys. Rev. Lett. **67**, 648 (1991).
[16] D. R. Nelson and V. M. Vinokur, Phys. Rev. B **48**, 13 060 (1993).
[17] J. R. Thompson, L. Krusin-Elbaum, D. K. Christen, K. J. Song, M. Paranthaman, J. L. Ullmann, J. Z. Wu, Z. F. Ren, J. H. Wang, J. E. Tkaczyk, and J. A. Deluca, Appl. Phys. Lett. **71**, 536 (1997).
[18] H. W. Weber and G. W. Crabtree, in *Studies of High Temperature Superconductors*, edited by A. V. Narlikar (Nova, New York, 1992), Vol. 9, p. 37.
[19] L. Krusin-Elbaum, D. Lopez, J. R. Thompson, R. Wheeler, J. Ullmann, C. W. Chu, and Q. M. Lin, Nature (London) **389**, 243 (1997).
[20] J. Schwartz, S. Nakamae, G. W. Raban Jr., J. K. Heuer, S. Wu, J. L. Wagner, and D. G. Hinks, Phys. Rev. B **48**, 9932 (1993).
[21] M. C. Frischherz, M. A. Kirk, J. Farmer, L. Greenwood, and H. W. Weber, Physica C **232**, 309 (1994).
[22] J. Karpinski, H. Schwer, R. Molinski, G. I. Meijer, K. Conder, E. Kopnin, J. Löhle, Ch. Rossel, D. Zech, J. Hofer, A. Wisniewski,

and R. Puzniak, in *Studies of High-Temperature Superconductors* (Ref. 18), Vol. 24, p. 165.
[23] H. W. Weber, H. Bock, E. Unfried, and L. R. Greenwood, J. Nucl. Mater. **137**, 236 (1986).
[24] C. Rossel, P. Bauer, D. Zech, J. Hofer, M. Willemin, and H. Keller, J. Appl. Phys. **79**, 8166 (1996).
[25] D. Zech, J. Hofer, H. Keller, C. Rossel, P. Bauer, and J. Karpinski, Phys. Rev. B **53**, R6026 (1996).
[26] D. E. Farrell, C. M. Williams, S. A. Wolf, N. P. Basal, and V. G. Kogan, Phys. Rev. Lett. **61**, 2805 (1988).
[27] Y. C. Kim, J. R. Thompson, D. K. Christen, Y. R. Sun, M. Paranthaman, and E. D. Specht, Phys. Rev. B **52**, 4438 (1995).
[28] G. Blatter, M. V. Feigel'man, V. B. Geshkenbein, A. I. Larkin, and V. M. Vinokur, Rev. Mod. Phys. **66**, 1125 (1994).
[29] J. R. Thompson, Yang Ren Sun, A. P. Malozemoff, D. K. Christen, H. R. Kerchner, J. G. Ossandon, A. Marwick, and F. Holtzberg, Appl. Phys. Lett. **59**, 2612 (1991).
[30] A. Schilling, H. R. Ott, and Th. Wolf, Phys. Rev. B **46**, 14 253 (1992).
[31] A. Schilling, R. Jin, J. D. Guo, H. R. Ott, I. Tanaka, and H. Kojima, Physica B **194-196**, 1555 (1994).
[32] J. Ricketts, R. Puzniak, C.-J. Liu, G. D. Gu, N. Koshizuka, and H. Yamauchi, Appl. Phys. Lett. **65**, 3284 (1994).
[33] T. Hanaguri, Y. Tsuchiya, S. Sakamoto, and A. Maeda, Phys. Rev. Lett. **78**, 3177 (1997).
[34] F. M. Sauerzopf, H. P. Wiesinger, H. W. Weber, and G. W. Crabtree, Phys. Rev. B **51**, 6002 (1995).
[35] F. M. Sauerzopf, Phys. Rev. B **57**, 10 959 (1998).
[36] D. Zech, C. Rossel, L. Lesne, H. Keller, S. L. Lee, and J. Karpinski, Phys. Rev. B **54**, 12 535 (1996).
[37] D. Zech, S. L. Lee, H. Keller, G. Blatter, B. Janossy, P. H. Kes, T. W. Li, and A. A. Menovsky, Phys. Rev. B **52**, 6913 (1995).